

ISSN 2281-4299



DIPARTIMENTO DI INGEGNERIA INFORMATICA  
AUTOMATICA E GESTIONALE ANTONIO RUBERTI



**SAPIENZA**  
UNIVERSITÀ DI ROMA

**Design Optimization of Synchronous  
Reluctance Motor for low Torque Ripple**

Andrea Cristofari  
Giuseppe Fabri  
Stefano Lucidi  
Francesco Rinaldi  
Francesco Romito  
Marco Santececca  
Marco Villani

Technical Report n. 10, 2017

# Design Optimization of Synchronous Reluctance Motor for low Torque Ripple

A. Cristofari, G. Fabri, S. Lucidi,  
F. Rinaldi, F. Romito, M. Santececca, M. Villani

**Abstract.** The aim of this paper is to optimize the design of multiple flux barriers Synchronous reluctance motor in order to smooth the torque profile without rotor skewing. A new strategy is proposed by modelling the particular optimal design problem as mixed integer constrained minimization of a suitable objective function. The procedure has allowed to optimize the rotor shape for minimum torque ripple starting from an existing stator core.

**Keywords:** Synchronous reluctance. Torque ripple optimization. Finite element analysis. Derivative-free algorithms. Nonlinear mixed-integer optimization methods.

---

Andrea Cristofari  
Department of Computer, Control and Management Engineering  
Sapienza University of Rome; via Ariosto, 25, 00185 Roma, Italy  
E-mail: cristofari@dis.uniroma1.it

Giuseppe Fabri.  
Department of Industrial and Information Engineering and Economy  
University of L'Aquila, 67100 L'Aquila, Italy  
E-mail: giuseppe.fabri@univaq.it

Stefano Lucidi  
Department of Computer, Control and Management Engineering  
Sapienza University of Rome; via Ariosto, 25, 00185 Roma, Italy  
E-mail: lucidi@dis.uniroma1.it

Francesco Rinaldi  
Department of Mathematics  
University of Padova; via Trieste, 63, 35121 Padova, Italy  
E-mail: rinaldi@math.unipd.it

Francesco Romito  
ACT Operations Research IT  
Sapienza University of Rome; via Ariosto, 25, 00185 Roma, Italy  
E-mail: francesco.romito@act-OperationsResearch.com

Marco Santececca  
Department of Industrial and Information Engineering and Economy  
University of L'Aquila, 67100 L'Aquila, Italy  
E-mail: msante@hotmail.it

Marco Villani  
Department of Industrial and Information Engineering and Economy  
University of L'Aquila, 67100 L'Aquila, Italy  
E-mail: marco.villani@ing.univaq.it

# 1 Introduction

Synchronous Reluctance Motors (SRM) could be considered as alternative to its counterparts, namely permanent magnet and induction motors and have advantages such as low cost and high efficiency. The transversally laminated rotor is preferable and exhibits a reduced inertia due to air-flux barriers (Fig.1).

The torque generated by SRM depends on the magnetic saliency of the rotor: no windings, brush or permanent magnets (PM) are used which makes the SRM a simple and robust electric machine.

Compared with permanent magnet machines, the SRM can operate at high speed because of the easier field weakening capability and the rugged rotor. If compared with induction motors it has theoretically no rotor losses and a comparable torque density depending on the design of the machine; moreover, the SRM has lower temperature rise in the rotor and shaft and consequently good efficiency and higher reliability.

On the other hand, synchronous reluctance machines usually present some additional issues like lower power factor but above all higher torque ripple that is intolerable in most of applications [1,2,3]: it is due to the interaction between the spatial harmonics of electrical loading and the rotor anisotropy and gives rise to noise and vibrations.

The easiest and commonly adopted solution for the torque ripple reduction is the skewing of the rotor stack (Fig.2). It could appear as a simple and cheap measure to actuate but gives rise some drawbacks. Particularly, a slight reduction of the output torque and then a difficulty in the insertion of permanent magnets inside the rotor core for the low cost PM-assisted SRM [4]. In this case, the continuous rotor skewing cannot be adopted and the alternative solution is a multi-stack rotor core where the rotor is split into two or more parts, each of them is skewed with respect to the others: this solution could be too expensive and not convenient to adopt from the industrialization point of view.

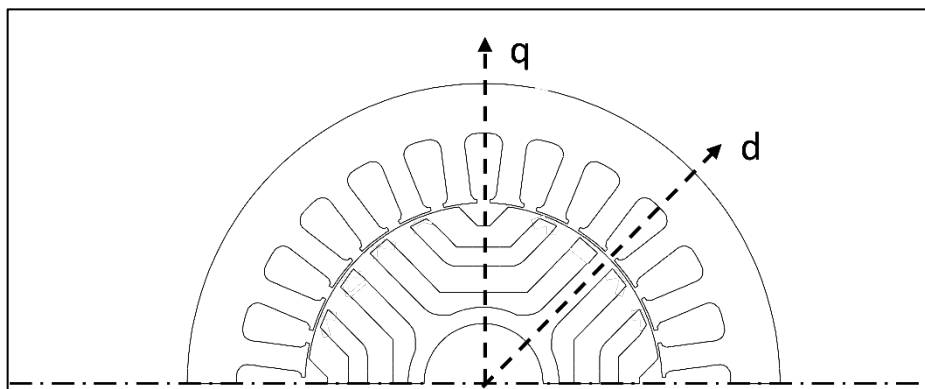


**Fig. 1.** Cross section of SRM with transversally laminated rotor (half machine).

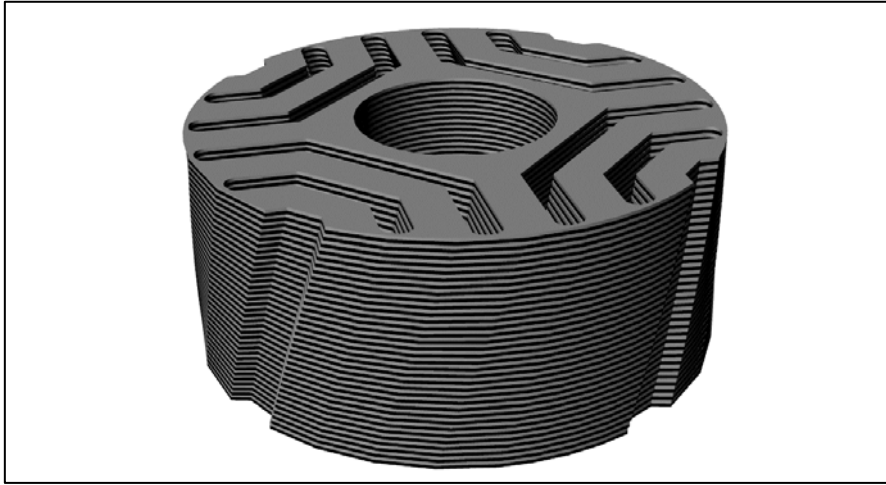


**Fig. 2.** SRM: 3D view of skewed rotor.

The design of the SRM requires a fine analysis and an accurate prediction of machine parameters and performances [5]. The reduction of torque ripple represents one of the most relevant constraints during the design step and the aim is to find a solution that allows to satisfy the requirements and simplify the motor assembling avoiding the skewing. This can be achieved by an appropriate combination of design parameters and a right choice of the number of flux barriers with respect to the stator slots.

This paper presents a novelty strategy to reduce the torque ripple of the synchronous reluctance motor by an innovative optimization algorithm. The focus is to smooth the torque profile by varying the dimensions of the rotor shape only without any change in the stator core and winding and above all without rotor skewing. For this, a commercial three-phase induction motor has been chosen substituting the squirrel cage rotor with a multiple flux-barriers one. The new rotor has been designed and then refined by the optimization algorithm in order to reduce the torque ripple.

## **2 The preliminary design of the SRM**

In this step, the preliminary design of the SRM has been carried out starting from a commercial three-phase induction motor (3kW, 4 pole, 400V, 50 Hz, TEFC, IEC size 100): Table 1 presents the motor requirements.

The same stator core and housing has been adopted, substituting the squirrel cage rotor with a flux-barriers one: this approach allows to minimize the investment costs in new tooling using existent components.

The design of SRM is mainly focused on the rotor creation and, more specifically, the type of flux barrier topology. For this, a sizing procedure has been used for the design of the rotor shape: it allows to determine the rotor dimensions (Fig.3) by adopting simplified relationships between geometrical and physical motor data in order to meet the specifications. These data allow to calculate the motor performance i.e. the axis fluxes, the magnetic potential differences, the flux densities, the axis currents, the power

factor and the torque. A detailed description of the sizing procedure is given in [6] and [7].

The sizing of rotor is not easy to carry out due to presence of the flux barriers whose number and dimensions affect heavily the *saliency ratio*, that is the ratio between  $d$  and  $q$ -axis inductances. For this reason, the authors have introduced several relationships among the rotor dimensions (Fig.3) and the rotor diameter ( $D_r$ ), by means of suitable coefficients ( $k_i$ ).

These relations and the coefficients have been refined and tested analyzing several SRMs, of different size, by the Finite

Element analysis. Therefore, these relations represent a guideline for the designer and should orient him towards the search of a good solution. For a rotor with two flux barriers they are (Fig. 3):

$$\begin{aligned}
 k_1 D_r &\leq fb1 \leq k_2 D_r \\
 k_3 D_r &\leq a1d \leq k_4 D_r \\
 k_5 D_r &\leq b_1 \leq k_6 D_r \\
 k_7 D_r &\leq b_2 \leq k_8 D_r \\
 fb2 &\geq k_9 fb1 \quad \text{and} \quad fb3 \geq k_{10} D_r
 \end{aligned}
 \tag{1}$$

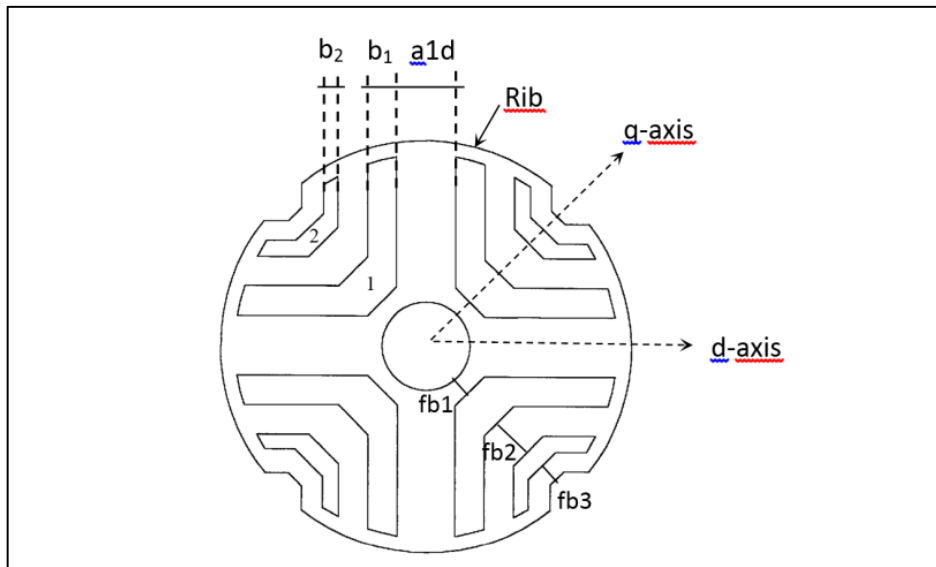


**Fig. 3.** Rotor dimensions.

This approach will be very useful for the next optimization step. In fact, the coefficients  $k_i$  are imposed in the Input data and these values define a range within each variable should vary according to the imposed values on  $D_r$ . The sizing process starts considering, for each variable, the average value and this choice allows to obtain a preliminary rotor design that certainly does not represent the final design. The design refinement is reached by the optimization algorithm (Section IV).

The number of flux barriers ( $N_{barr}$ ) has been calculated according to the number of stator slots ( $N_{slot}$ ) and the following relationship:

$$(N_{barr})_{TOT} = N_{pole} K_s, \quad (2)$$

where  $N_{pole}$  is the number of poles and

$$K_s \neq \frac{N_{slot}}{N_{pole}}. \quad (3)$$

It is import to underline that increasing the number of flux-barriers, the torque tends to increase whereas the torque ripple decreases.

Since the chosen stator core presents 36 slots, 24 barriers have been chosen according to the (2) and particularly 6 barriers per pole: this choice has also been conditioned by the constraint on the outer rotor diameter.

The cross section of the preliminary design is shown in Fig.4. This configuration is a quite conventional reluctance geometry, characterized by three flux barriers that share the same width, tilt angle and distance between them. Also the barrier fillet radius at the external rib is the same. An external channel located along the q-axis has been considered, in order to simplify the welding procedure of the rotor stack.

About the thickness of ribs (Fig.3) they should be chosen according to the improvement of saliency ratio and the mechanical strength. From a preliminary analysis a minimum value of 1 mm has been imposed: this value is consistent with the maximum speed and mechanical stress.

The preliminary design has been analyzed by the Finite Element (FE) software, since the SRM presents notable non-linear characteristics due to the effects of the saturation and cross-coupling phenomena. An accurate bi-dimensional FE model has been developed introducing a parametric model in order to modify any geometric dimensions of the rotor shape.

A transient analysis has been carried out and one pole has been simulated thanks you the motor symmetry.

**Table 1.** Motor requirements

Rated power	kW	3.0
Rated speed	rpm	1500
Rated torque	Nm	19
Number of poles		4
Number of slots		36
Outer stator diameter	mm	150
Inner stator diameter	mm	90
Stack length	mm	150
Airgap length	mm	0.50
Electrical steel		M470-50A
Cooling		air cooled

The behavior of the electromagnetic torque, as a function of the rotor position, has been calculated by a series of time-based simulations: then its average value along the entire electrical period has been evaluated. More in the detail, it can be proved that for the considered combination  $N_{slot}/N_{parr}$ , the electrical period of the torque is equal to 60 el.deg. (30 mech.deg.). In turn, each transient analysis consist of 80 computational steps, which means that the electromagnetic torque is represented with an accuracy of 0.75 el.deg.

We performed the time stepping FE simulations (at 1500 rpm) by imposing the axis currents in order to maximize the torque-current ratio: moreover, a conventional temperature of 75°C has been chosen for the stator winding. Table 2 presents the main data and performance of the preliminary design and Fig.5 the torque profile. The torque ripple, defined like as the ratio between the difference of the maximum and minimum values of torque and the average one is about 20% for the no-skewed rotor. Moreover, a further analysis has been carried out with a skewed rotor in order to verify the effect on the torque behavior: a continuous rotor skewing has been simulated with the skewing angle equal to the stator slot angle. Fig.6 presents the new torque profile: in this case, the average torque is 18.3 Nm and the ripple 8.1% with a reduction of about 60% respect to the no-skewed rotor.

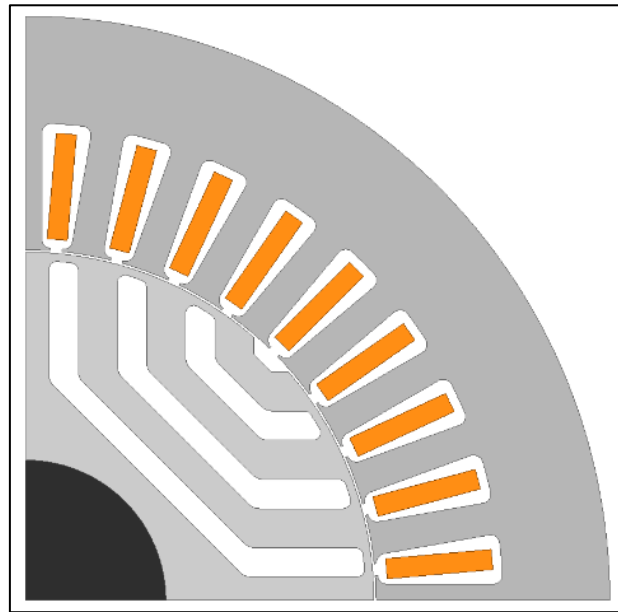


**Fig. 4.** Cross-section of the preliminary design (1 pole).

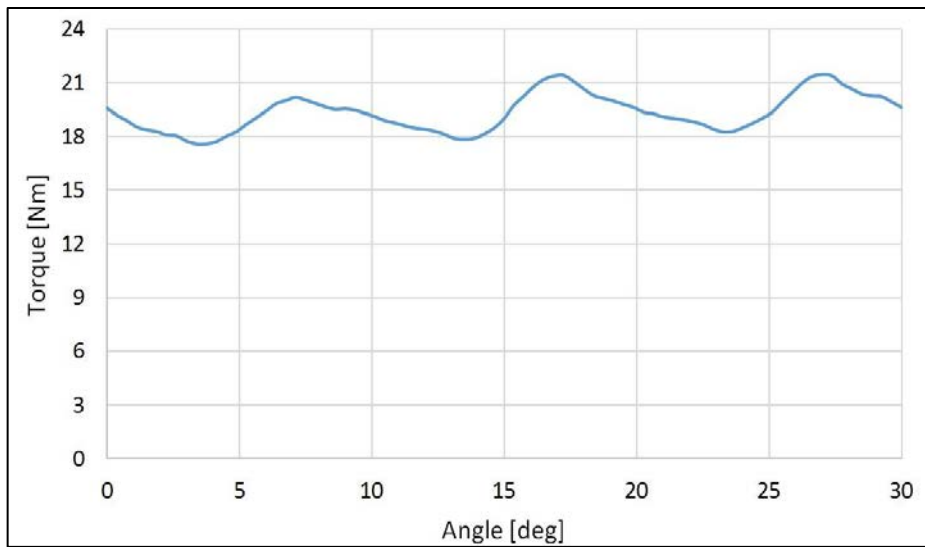


**Fig. 5.** Preliminary design: torque behavior (no-skewed rotor).

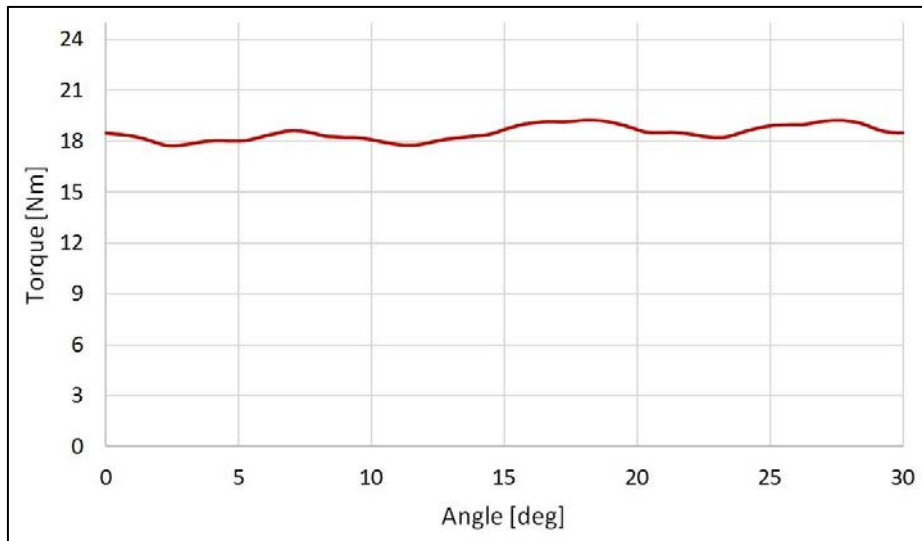


**Fig. 6.** Preliminary design: torque behavior (skewed rotor).

**Table 2.** Main data and performance of the preliminary design

Outer stator diameter	mm	150
Inner stator diameter	mm	90
Stack length	mm	150
N.turns per phase		180
Wire size	mm <sup>2</sup>	1.135
N.barriers per pole		6
Width of the rotor tooth along d-axis (a1d)	mm	6
Thickness of rotor ribs	mm	1
Width of barrier_1 (b1)	mm	3
Width of barrier_2 (b2)	mm	3
Width of barrier_3 (b3)	mm	3
Performance		
Phase voltage	V <sub>rms</sub>	220
Phase currents	A <sub>rms</sub>	6.5
Average torque	Nm	19.3
Base speed	rpm	1500
Phase resistance @ 75°C	Ω	1.78
Joule losses	W	226
Iron losses	W	81
Efficiency	%	90.1
Torque ripple (no-skewed)	%	20.1

### 3 Design Optimization of the SRM

The demand of high-performance motors requires the definition of more efficient designs. This aim can be achieved by interfacing the Finite Element software with automatic optimization procedures [8].

In particular the FE analysis can be used to evaluate the motor performance, namely to compute the objective function value and some of the constraints. The optimization procedure can use the information obtained by the FE program to iteratively update the set of motor parameters and try to identify an “optimal” motor by making a trade-off between the different parameters of the machine.

The set of parameters  $\mathbf{x}$  used in the optimization procedure of the SRM concern the rotor shape only and are listed in Table 3. Fig. 7 shows in details the 26 design variables (dimensions of flux barriers, tilt angles, fillet radii): they have been varied according to practical limits existing in cutting the rotor shape.

Moreover, several constraints have been introduced to guarantee the reliability and feasibility of the final design (Table 4). They are: the average torque, the maximum flux densities in the stator and rotor core and the percentage of torque ripple.

The aim of the optimization was to refine the rotor shape, without skewing, in order to smooth the torque profile in the electrical period. This approach has required many FE calls for each optimization step and high

computation time, but represents a powerful tool for an accurate design of the machine.

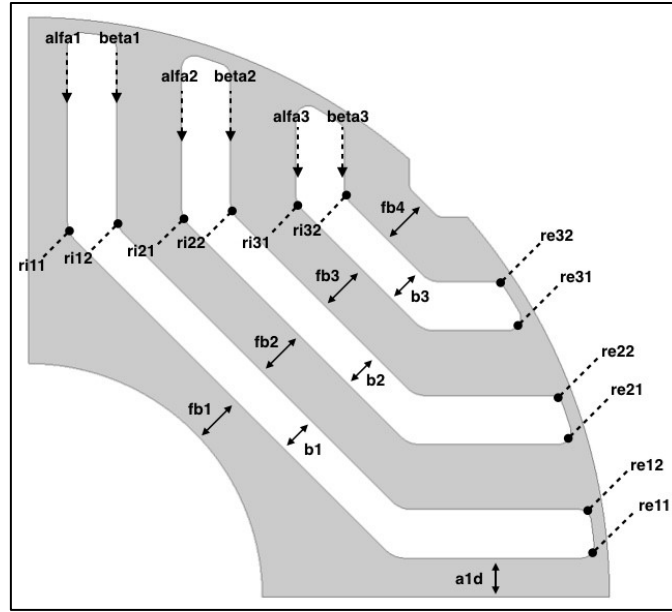


**Fig. 7.** Rotor independent variables.

**Table 3.** Minimum and Maximum Ranges of Design Variables

Variables		min	max
x <sub>1</sub> . Width of rotor tooth along d-axis (mm)	a1d	4	8
x <sub>2</sub> . Width of barrier <sub>1</sub>	b <sub>1</sub>	2	4.5
x <sub>3</sub> . Width of barrier <sub>2</sub>	b <sub>2</sub>	2	4.5
x <sub>4</sub> . Width of barrier <sub>3</sub>	b <sub>3</sub>	2	4.5
x <sub>5</sub> . Distance between shaft and barrier <sub>1</sub>	fb <sub>1</sub>	2	3
x <sub>6</sub> . Distance between barriers 1-2	fb <sub>2</sub>	3	5
x <sub>7</sub> . Distance between barriers 2-3	fb <sub>3</sub>	3	5
x <sub>8</sub> . Distance between barriers 3-ext.channel	fb <sub>4</sub>	3	5
x <sub>9</sub> ÷ x <sub>10</sub> Tilt angles barrier <sub>1</sub>	$\alpha_1, \beta_1$	0°	5°
x <sub>11</sub> ÷ x <sub>12</sub> Tilt angles barrier <sub>2</sub>	$\alpha_2, \beta_2$	0°	5°
x <sub>13</sub> ÷ x <sub>14</sub> Tilt angles barrier <sub>3</sub>	$\alpha_3, \beta_3$	0°	5°
x <sub>15</sub> ÷ x <sub>16</sub> Fillet radii (mm)	ri, re	0.5	3

**Table 4.** Constraints

Constraints		Limits
c1. Max flux density in the stator tooth	T	≤ 1.60
c2. Max flux density in the stator yoke	T	≤ 1.45
c3. Max flux density in the rotor tooth	T	≤ 1.50
c4. Torque ripple	%	≤ 10.0
c5. Average torque @ 1500 rpm	Nm	≥ 19.0

## 4 The Optimization Algorithm

The above described design problem can be modeled by an optimization problem, where the functions describing the motor behavior with respect to its parameters are unknown and they can be only computed by complex simulation programs. So, the derivatives of these functions are unknown as well, and then, a derivative-free algorithm must be employed.

A further difficulty arising in our context is the high computational burden needed to evaluate the motor behavior in the entire electrical period.

Moreover, the aim of the minimization procedure is twofold: on the one hand, the torque profile must be smoothed, and, on the other hand, its average value must be maximized. So, a multiobjective problem could be in principle introduced.

Several multiobjective derivative-free methods have been proposed in the literature (see e.g. [9, 10, 11] and references therein for further details). Some of those methods take into account preferences of the decision maker (i.e. the person that can give preference information concerning the solutions) relating the objectives.

As we said, in the considered context there is usually the need for a trade-off between a high expected value of the torque profile and a small torque profile variance.

For any motor parameter vector  $x$ , we indicate with  $a(x)$  and  $\sigma(x)$  the expected value and the standard deviation of the torque profile in the electrical period, respectively. One way we have to properly take standard deviation into account is to minimize a proper combination of the two objectives, that is,

$$f(x) = -a(x) + \gamma\sigma(x),$$

thus obtaining a "risk-sensitive" objective function.

The parameter  $\gamma \geq 0$  is called *risk-aversion parameter*, since it sets the relative values of torque profile standard deviation and expected value (for  $\gamma > 0$ , we are willing to trade off a decrease in the expected value of the torque profile for a sufficiently large decrease in the torque profile standard deviation). In our case, we set the risk-aversion parameter  $\gamma = 10^4\sqrt{N}$ , where  $N$  is the number of measures in the electrical period (i.e.,  $N = 61$ ).

In particular, we deal with the following mixed integer non-linear minimization problem:

$$\begin{aligned} & \min f(x) \\ & g(x) \leq 0 \\ & l \leq x \leq u \\ & x_i \in Z, \quad i \in I_z \\ & x_i \in R, \quad i \in I_c = \{1, \dots, n\} \setminus I_z, \end{aligned} \tag{4}$$

where  $f: R^n \rightarrow R$ ,  $g: R^n \rightarrow R^m$ ,  $x \in R^n$ ,  $l \in R^n$ ,  $u \in R^n$ ,  $I_z$  is the index set of the integer variables and  $I_c$  is the index set of the continuous variables.

In problem (4),  $x$  is the motor parameter vector and the constraints are those described in the previous section.

Recalling the considerations made above on the computational burden needed to evaluate the objective function, using a global optimization algorithm (e.g. [12, 13]) can be prohibitive.

So, we employ a local derivative-free algorithm to solve problem (4). In particular, we use *Algorithm DFL*, recently proposed in [14], which is based on a sequential penalty approach. Namely, the non-linear constrained problem (4) is approximated by a sequence of box-constrained problems of the form:

$$\begin{aligned} \min P(\mathbf{x}; \epsilon_k) = & f(\mathbf{x}) + \frac{1}{\epsilon_k} \sum_{i=1}^m \max\{0, g_i(\mathbf{x})\}^p \\ & l \leq \mathbf{x} \leq u \\ & x_i \in Z, \quad i \in I_Z \\ & x_i \in R, \quad i \in I_C, \end{aligned} \quad (5)$$

where  $\epsilon_k > 0$  and  $p > 1$ .

Algorithm DFL generates a sequence  $\{\epsilon_k\}$  such that, for any given  $\epsilon_k$ , function  $P(\mathbf{x}; \epsilon_k)$  is reduced (with respect to  $\mathbf{x}$ ) by means of suitable derivative-free line searches along all coordinate directions. Afterwards, if the constraint violation at the new point is not sufficiently decreased, then the penalty parameter  $\epsilon_k$  is updated.

We report in Figure 8 a scheme of Algorithm DFL, highlighting the main steps of the method.

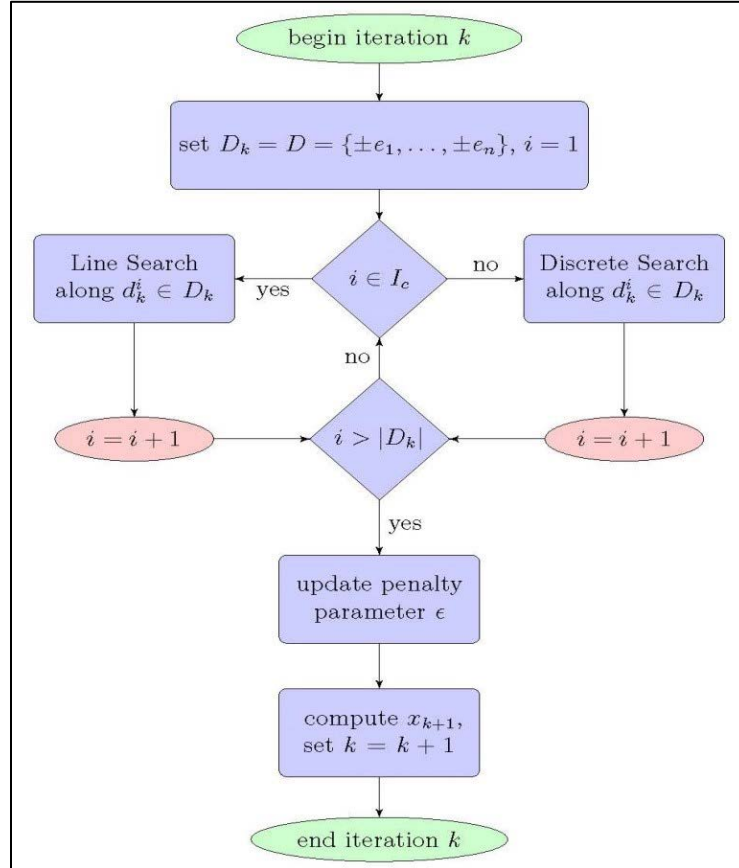


**Fig. 8.** Algorithm DFL.

A more detailed description of the algorithm and the analysis of its theoretical properties can be found in [13]. Moreover, a Fortran 90 code of Algorithm DFL is freely available for download from the web page <http://www.dis.uniroma1.it/~lucidi/DFL>.

As we can see by taking a look at the scheme, the method is based on a suitable sampling strategy along a specific set of search directions  $D = \{\pm e_i\}$ . It means that, by exploring a given direction, we move in a component-wise fashion.

Hence, we can use a specific search strategy (Continuous/Discrete) depending on the direction (component) we choose. When moving a continuous variable, the goal is guaranteeing both a sufficiently large movement along the search direction and a sufficient decrease in the objective function. When dealing with discrete variables, we further want to sample the objective function in such a way that integrality is always satisfied. At each iteration, after all directions have been explored, we check if an updating of the penalty parameter is timely and, finally, we update the iterate.

The sampling strategy is able to get, in the limit, sufficient knowledge of the problem functions (by using the Continuous and Discrete search) to recover both first order information for the continuous variables and some sort of local optimality for the discrete ones.

For what concerns the termination criterion, we arrested the algorithm when it produced a trial stepsize  $\alpha^k = 10^{-6}$ .

Now, we show the numerical results achieved by Algorithm DFL. The number of iterations and function evaluations required to solve the problem are equal to 1000 and 1697, respectively. The final value of the torque is 20.00 with a standard deviation 0.30 and a constraint violation of  $4 \cdot 10^{-2}$ .

In Figure 9, 10 and 11, we focus on its computational behavior by reporting the value of the average torque, the standard deviation of the torque profile and the constraint violation (i.e.,  $\sum_{i=1}^m \max\{0, g_i(x^k)\}$ ) versus iteration  $k$ , respectively.

More in detail, the figures show that after 120 iterations (corresponding to 208 function evaluations) the algorithm is able to find an efficient solution, with an average torque equal to 19.89, a standard deviation of torque profile equal to 0.38 and a constraint violation equal to 0.32.

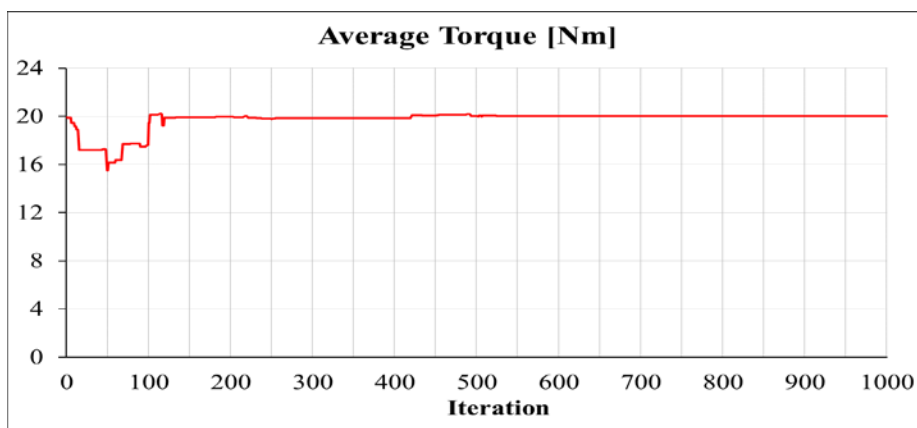


**Fig. 9.** Behavior of the average torque during the minimization by Algorithm DFL.

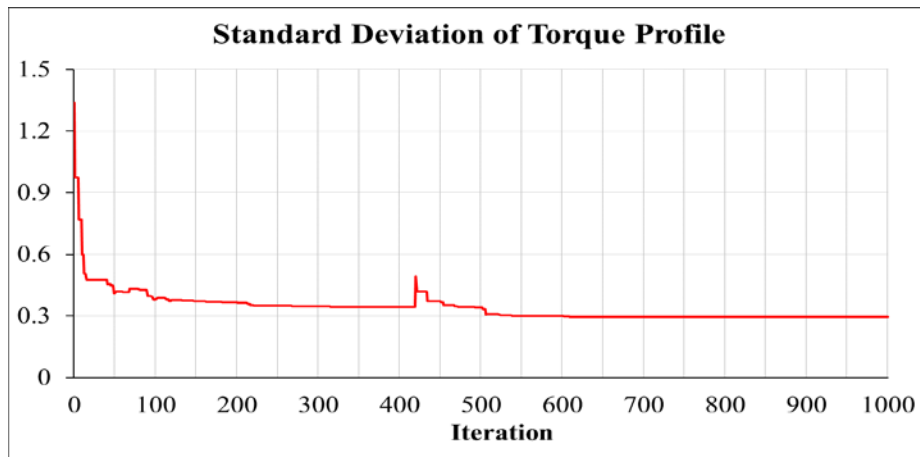


**Fig. 10.** Behavior of the standard deviation of torque profile during the minimization by Algorithm DFL.

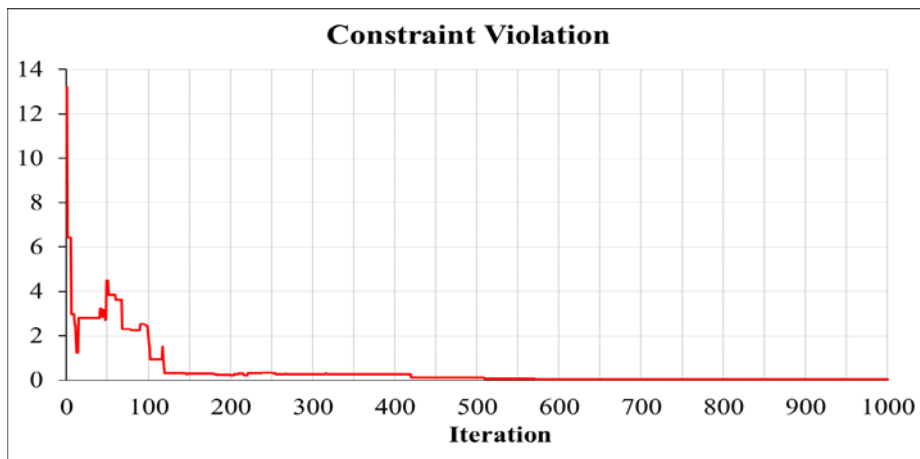


**Fig. 11.** Behavior of the constraint violation DFL during the minimization by Algorithm DFL.

Finally, to evaluate the possible limits and drawbacks of using a local algorithm, we also tried a global algorithm. In particular, we considered an extension of CMA-ES Algorithm for mixed integer problems [15, 16], downloaded from [https://www.lri.fr/~hansen/cmaes\\_inmatlab.html](https://www.lri.fr/~hansen/cmaes_inmatlab.html). Default parameters were used and the algorithm was stopped after 10000 function evaluations. The inequality constraints  $g_i(x) \leq 0$  were handled as in Algorithm DFL, that is, they were added to the objective function as a penalty term weighted by a parameter  $\epsilon_k$ , updated as described above for Algorithm DFL.

In Table 5, we report the final results achieved by CMA-ES, compared with those obtained by DFL.

**Table 5.** Comparison between DFL and CMA-ES

	AVERAGE TORQUE	STANDARD DEVIATION	CONSTRAINT VIOLATION
DFL	20	0.30	4E-2
CMA-ES	5.33	0.13	14.74

Table 5 seems to indicate that the global strategy implemented in CMA-ES needs a large number of function evaluations to locate a satisfying solution, especially for what concerns feasibility. Moreover, the results reported in the table show that, even with a limited budget of evaluations, the DFL method is able to get good points both in terms of objective function values and feasibility. The comparison with CMA-ES further indicates that the way DFL handles constraints and integer variables is efficient and, in this specific context, guarantees much better performances.

## 5 Results

The main data of the optimized design are shown in Table 6: it includes some of the key machine dimensions and performance at 1500 rpm. The same phase current of previous analysis has been imposed. This design fully satisfies the constraints.

The cross-section of the new rotor is shown in Fig. 12. The comparison with the preliminary design (Fig.4) points out a difference on the flux barriers dimensions and a slight weight reduction of rotor core (about 7%): this allows to reduce the inertia of the machine that could be very useful if high dynamic performance are required.

The torque profile (no-skewed rotor) is shown in Fig. 13 and the ripple is 6.67%: this behavior can be compared with the curve shown in Fig. 6 (skewed rotor). Moreover, the axis inductances have been determined and in Fig. 14 are shown the profiles: from these curve the average saliency ratio has been evaluated and it is about 6.4.

Fig. 15 presents the flux density distribution where the maximum values in the stator teeth and yoke are fully consistent with the imposed constraints (Table 6).

In Table 7 are compared the main performance of the proposed solutions. The torque ripple of the optimized design is lower than the preliminary design one with skewed rotor, and the average torque is slightly higher. Respect to the preliminary design without skewing, the new motor presents a significant ripple reduction of about 67%.

A further analysis has been carried out to determine the flux weakening capability of the optimized design. Fig. 16 shows the torque versus speed of the machine.

All these results are quite satisfactory and confirm the goodness of the optimization procedure and the effectiveness of the proposed approach.

The aim was to smooth the torque profile by varying the dimensions of the rotor shape only without any change in the stator core and winding and above all without rotor skewing.

The results have demonstrated that this aim has been fully reached. The new design is a simple and cheap solution to industrialize and it is suitable

for the insertion of proper amount of permanent magnets in the flux barriers for the low cost PM-assisted SRMs.

Nevertheless, the study can be extended to consider also independent variables for the stator core, resulting in a whole motor optimization.

**Table 6.** Main data and performance of the optimized design

Outer stator diameter	mm	150
Inner stator diameter	mm	90
Stack length	mm	150
N. barriers per pole		6
Width of the rotor tooth along d-axis (a1d)	mm	5.78
Thickness of rotor ribs	mm	1
Width of barrier_1 (b1)	mm	3.06
Width of barrier_2 (b2)	mm	3.16
Width of barrier_3 (b3)	mm	4.46
Distance between shaft and barrier_1 (fb1)	mm	2.19
Distance between barriers 1-2 (fb2)	mm	4.16
Distance between barriers 2-3 (fb3)	mm	4.08
Performance		
Phase voltage	V <sub>rms</sub>	220
Phase currents	A <sub>rms</sub>	6.5
Current angle	°	65
Average torque	Nm	20
Rated speed	rpm	1500
Phase resistance @ 75°C	Ω	1.78
Joule losses	W	226
Iron losses	W	78
Efficiency	%	90.0
Power factor		0.81
Torque ripple (no-skewed)	%	6.67

**Table 7.** Performance of the proposed solutions

		Preliminary		Optimized
		no-skewed	skewed	no-skewed
Phase current	A <sub>rms</sub>	6.5	6.5	6.5
Average torque	Nm	19.3	18.3	20
Torque ripple	%	20.1	8.1	6.67

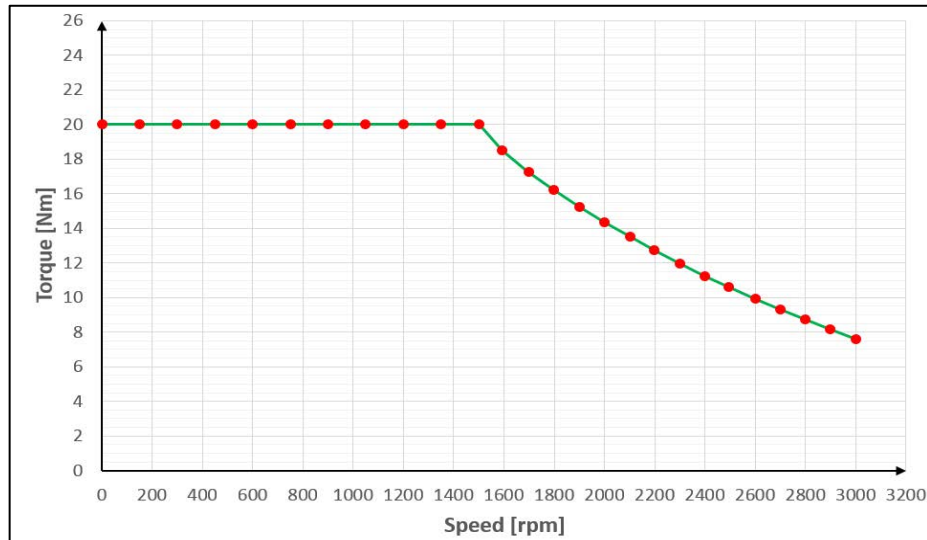


Fig. 12. Optimized design: torque vs. speed.

## 6 Conclusions

A novelty strategy to reduce the torque ripple of the synchronous reluctance motor has been presented. The focus was to smooth the torque profile by varying the dimensions of the rotor shape only without any change in the stator core and winding and above all without rotor skewing. For this, a commercial three-phase induction motor has been chosen substituting the squirrel cage rotor with a multiple flux-barriers one. The new rotor has been designed and then refined by an optimization algorithm. A new strategy has been proposed by modelling the particular optimal design problem as mixed integer constrained minimization of a suitable objective function.

## References

- [1] A. Vagati, M. Pastorelli, G. Franceschini, and S. C. Petrace, "Design of low-torque-ripple synchronous reluctance motors," *IEEE Trans. Ind. Appl.*, vol. 34, no. 4, pp. 758–765, Jul./Aug. 1998.
- [2] T.M Jahns and W. Soong, "Pulsating torque minimization techniques for permanent magnet ac motor drives: a review!", *IEEE Trans. on Industrial Electronics*, IE43(2), 321-330, April 1996.
- [3] R. Moghaddam, F. Magnussen, C. Sadarangani, "Novel Rotor Design Optimization of Synchronous Reluctance Machine for Low Torque Ripple", ICEM 2012, XX International Conference on Electrical Machines, Marsiglia (France), September 2012.

- [4] M. Barcaro and N. Bianchi, "Interior PM machines using ferrite to substitute rare-earth surface pm machines," in 20th International Conference on electrical Machines (ICEM), 2012, pp. 1339–1345.
- [5] I. Boldea, *Reluctance Synchronous Machines and Drives*, Clarendon Press: Oxford, 1996.
- [6] F. Parasiliti, M. Villani, "Synchronous reluctance motors design and performance prediction using an analytical procedure", *Electrical Engineering and Electromagnetics*, WIT Press, 2003, ISBN- 1-85312-981-X, pp. 147-156.
- [7] F.Parasiliti, M.Villani "Magnetic analysis of flux barriers Synchronous Reluctance Motors" ICEM 2008, XVIII International Conference on Electrical Machines, Vilamoura (Portugal), September 2008.
- [8] F. Parasiliti, M. Villani, S. Lucidi, F. Rinaldi, "Finite Element Based Multi-Objective Design Optimization Procedure of Interior Permanent Magnet Synchronous Motors for Wide Constant-Power Region Operation". *IEEE Trans. on Industrial Electronics*, vol. 59, n. 6, June 2012.
- [9] C. Audet, G. Savard, W. Zghal, "Multiobjective optimization through a series of single-objective formulations". *SIAM Journal on Optimization*, 19(1):188–210, 2008.
- [10] G. Liuzzi, S. Lucidi, F. Rinaldi, "A Derivative-Free Approach to Constrained Multiobjective Nonsmooth Optimization", *SIAM Journal on Optimization*, vol. 26(4), pp. 2744–2774, 2016.
- [11] A. L. Custódio, J. F. A. Madeira, A. I. F. Vaz, L. N. Vicente, "Direct multisearch for multiobjective optimization", *SIAM Journal on Optimization*, 21, pp. 1109–1140, 2011.
- [12] R. Paulavičius, Ya. D. Sergeyev, D.E. Kvasov, J. Žilinskas, "Globally-biased DISIMPL algorithm for expensive global optimization", *Journal of Global Optimization*, 59(2-3), pp. 545–567, 2014.
- [13] G. Liuzzi, S. Lucidi, V. Piccialli, "Exploiting derivative-free local searches in DIRECT-type algorithms for global optimization", *Computational Optimization and Applications*, pp. 1–27, 2015.
- [14] G. Liuzzi, S. Lucidi, F. Rinaldi, "Derivative-Free Methods for Mixed-Integer Constrained Optimization Problems", *Journal of Optimization Theory and Applications*, vol. 164, pp. 933–965, 2015.
- [15] Hansen, N. "A CMA-ES for mixed-integer nonlinear optimization", Technical Report RR-7751, INRIA, 2011.
- [16] Hansen, N. "The CMA evolution strategy: a comparing review", Towards a new evolutionary computation, Springer Berlin Heidelberg, pp. 75-102, 2006.